



Quasi 18 h wave activity in ground-based observed mesospheric H₂O over Bern, Switzerland

Martin Lainer¹, Klemens Hocke^{1,2}, Rolf Rufenacht^{1,a}, and Niklaus Kämpfer^{1,2}

¹Institute of Applied Physics, University of Bern, Bern, Switzerland

²Oeschger Center for Climate Change Research, University of Bern, Bern, Switzerland

^anow at: Leibniz Institute of Atmospheric Physics, Kühlungsborn, Germany

Correspondence: Martin Lainer (martin.lainer@iap.unibe.ch)

Received: 24 November 2016 – Discussion started: 11 January 2017

Revised: 9 November 2017 – Accepted: 13 November 2017 – Published: 18 December 2017

Abstract. Observations of oscillations in the abundance of middle-atmospheric trace gases can provide insight into the dynamics of the middle atmosphere. Long-term, high-temporal-resolution and continuous measurements of dynamical tracers within the strato- and mesosphere are rare but would facilitate better understanding of the impact of atmospheric waves on the middle atmosphere. Here we report on water vapor measurements from the ground-based microwave radiometer MIAWARA (MIddle Atmospheric Water vapor RAdiometer) located close to Bern during two winter periods of 6 months from October to March. Oscillations with periods between 6 and 30 h are analyzed in the pressure range 0.02–2 hPa. Seven out of 12 months have the highest wave amplitudes between 15 and 21 h periods in the mesosphere above 0.1 hPa. The quasi 18 h wave signature in the water vapor tracer is studied in more detail by analyzing its temporal evolution in the mesosphere up to an altitude of 75 km. Eighteen-hour oscillations in midlatitude zonal wind observations from the microwave Doppler wind radiometer WIRA (WInd RAdiometer) could be identified within the pressure range 0.1–1 hPa during an ARISE (Atmospheric dynamics Research InfraStructure in Europe)-affiliated measurement campaign at the Observatoire de Haute-Provence (355 km from Bern) in France in 2013. The origin of the observed upper-mesospheric quasi 18 h oscillations is uncertain and could not be determined with our available data sets. Possible drivers could be low-frequency inertia-gravity waves or a nonlinear wave–wave interaction between the quasi 2-day wave and the diurnal tide.

1 Introduction

The dynamics of the middle atmosphere are controlled by a broad spectrum of waves. Knowledge about the wave characteristics and incidence is important, not only to better understand the elements of middle-atmospheric dynamics also to improve predictions of weather (Hardiman et al., 2011) and climate (Orr et al., 2010) models. The latter are getting more important since the social impact of severe-weather events and climate change is increasing.

Waves with horizontal wavelengths reaching thousands of kilometers and showing periods up to several weeks are classified as planetary waves. A well-known class of planetary waves are Rossby waves (Salby, 1981b). Their periods range from 2 to approximately 18 days in the middle atmosphere, showing strong interannual variability (Jacobi et al., 1998). Investigations of the quasi 2-day wave are found for instance in studies by Salby (1981a), Rodgers and Prata (1981) and Yue et al. (2012), and more recently by Tschanz and Kämpfer (2015), who analyzed the 2-day wave signatures in Arctic middle-atmospheric water vapor measurements in conjunction with the occurrence of sudden stratospheric warmings. Characteristics of the 5-day wave were analyzed by Rosenlof and Thomas (1990), Wu et al. (1994), Riggan et al. (2006) and Belova et al. (2008), and waves with even longer periods have been observed in the mesosphere and lower thermosphere (Forbes et al., 1995; McDonald et al., 2011; Scheiben et al., 2014; Rufenacht et al., 2016).

Besides the presence of planetary waves, signatures of atmospheric tides (ter-diurnal, semi-diurnal, diurnal) can be seen in middle-atmospheric constituents or parameters like wind, ozone, water vapor or temperature. Diurnal tides can

be triggered by latent heat release within the troposphere (Hagan and Forbes, 2002) and can be of migrating or non-migrating nature. Overall complex interactions of atmospheric waves and coupling processes between different atmospheric layers exist. As Forbes (2009) assessed, the semi-diurnal solar thermal tide is a feature in the atmosphere of the earth, and it serves to globally couple the troposphere, stratosphere, mesosphere, thermosphere and ionosphere.

Apart from direct observations of middle-atmospheric wind as a proxy for dynamical patterns, it is common to use observations of H₂O that can serve as diagnostic and dynamical tracers, even from ground-based profile measurements (Liu et al., 2013; Lainer et al., 2015), due to their relative long chemical lifetime, which is on the order of weeks in the mesosphere (Brasseur and Solomon, 2006).

Here we report on ground-based observed water vapor oscillations in the mesosphere above Switzerland (46.88° N, 7.46° W) with a period of around 18 h and investigate the monthly mean and temporal characteristics of the wave amplitudes. This is to our knowledge the first study that explores a quasi 18 h dominant wave mode in wintry (Northern Hemisphere) upper-mesospheric conditions with passive microwave radiometric techniques. For this investigation not only ground-based water vapor data are analyzed. A mesospheric zonal wind data set from a measurement campaign at the Observatoire de Haute-Provence (OHP, 43.56° N, 5.43° E) in France with the microwave Doppler wind radiometer WIRA (WInd RAdiometer; Rüfenacht et al., 2014) is also considered. The focus of this paper is on the observation of atmospheric wave signatures and their temporal evolution.

In Sect. 2 the data sets from the ground-based remote-sensing instruments are described. The data processing methodology and the underlying numerical approach are part of Sect. 3. Section 4 describes and analyzes the results and some distinguished features of the present 18 h spectral component. Possible implications of the observed wave activity in our H₂O and wind data, like an impact of inertia-gravity waves or a coupling of a quasi 2-day wave to the diurnal tide, are addressed in Sect. 4.3. Final conclusions are provided in Sect. 5.

2 Instruments and data sets

The advantage of ground-based microwave radiometry is that it can continuously measure the amount of atmospheric trace gases at altitudes between roughly 30 and 80 km under most environmental conditions. Observations are possible during day, night and cloudy conditions. The technique is widely used to study the middle atmosphere (Kämpfer et al., 2012). In this section we present the middle-atmospheric water vapor radiometer MIAWARA (MIddle Atmospheric Water vapor RAdiometer) and Doppler wind radiometer WIRA.

2.1 Middle-atmospheric water vapor radiometer

The middle-atmospheric water vapor radiometer MIAWARA was built in 2002 at the University of Bern (Deuber et al., 2004). The front end of the radiometer receives emissions from the pressure-broadened rotational transition line of the H₂O molecule at the center frequency of 22.235 GHz. For studying oscillations with periods shorter than 1 day, a high temporal resolution of a few hours with an evenly spaced time series is required. In our case a MIAWARA water vapor retrieval version with a temporal resolution of 3 h is applied. The H₂O retrieval from the integrated raw spectra is based on the optimal estimation method (OEM) as presented in Rodgers (2000). We use the ARTS/QPACK software (Eriksson et al., 2005, 2011), where the OEM is used to perform the inversion of the Atmospheric Radiative Transfer Simulator (ARTS). The FFT (fast Fourier transform) spectrometer in the back end of MIAWARA has a resolution of 60 kHz and the retrieval uses an overall spectrum bandwidth of 50 MHz. A monthly mean zonal mean Aura Microwave Limb Sounder (MLS) climatology provides the a priori water vapor profile, and additionally Aura MLS is used to set the pressure, temperature and geopotential height in the retrieval part. MIAWARA is part of NDACC (Network for the Detection of Atmospheric Composition Change) and has been persistently probing middle-atmospheric H₂O from the atmospheric remote sensing observatory in Zimmerwald (46.88° N, 7.46° E, 907 m a.s.l.), close to Bern, since 2006. In the stratosphere the vertical resolution of the water vapor profiles is 11 km and degrades to about 14 km in the mesosphere (Deuber et al., 2005). A recent validation against the Aura MLS v4.2 water vapor product (Livesey et al., 2015) revealed that for most months and altitudes the relative differences between MIAWARA and Aura MLS are below 5 % (Lainer et al., 2016).

During the winter months the tropospheric humidity is lower than during summer, and in consequence the microwave signal from the middle atmosphere is less attenuated by penetrating the troposphere to the ground-based receiver. Hence an integration of the signal of only 3 h can be used to retrieve the H₂O profiles. In order to characterize a retrieved H₂O profile, the averaging kernel matrix can be used (Rodgers, 2000). This key quantity describes to what extent the retrieval is smoothing the true atmospheric state and how sensitive it is to the a priori profile (measurement response). To define a reliable altitude range for our retrieved data, we use a typical range for the threshold for the measurement response between 60 and 80 %.

The MIAWARA H₂O time series between October 2014 and March 2016 is shown in Fig. 1 with a measurement response of 80 % that is represented by the white horizontal lines. Except for some outliers we consider the upper measurement limit to range within 0.02–0.04 hPa during the winter time period. In the summer season the H₂O retrieval from a 3 h signal integration has a significantly lower measurement response. It is not possible to get information that is suffi-

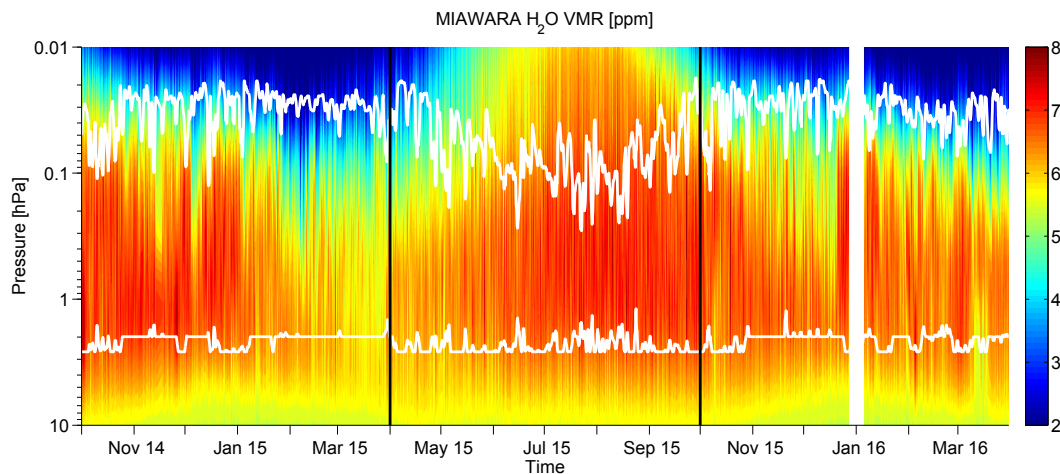


Figure 1. The water vapor volume mixing ratio (ppm) time series measured by MIAWARA between October 2014 and March 2016. The horizontal white lines indicate at which pressure levels the measurement response drops below 80 %. During the more humid and warm season between April and September 2015 the data will not be used. This is marked by the vertical black lines. A measurement gap occurred between 28 December 2015 and 4 January 2016 as shown by the white bar.

ciently a priori independent above approximately 0.1 hPa in the upper mesosphere. Further, we note that we are missing 1 week of MIAWARA data due to hardware problems beginning in the end of December 2015. This data gap is shown by a white bar in the MIAWARA H₂O time series.

In order to provide more information on the water vapor variability in the upper mesosphere, Figs. 2 and 3 are shown. There the monthly water vapor time series of MIAWARA averaged between 0.02 and 0.1 hPa are plotted during the two winter time periods. It is the same altitude region where the 18 h oscillations appeared. Later in the spectral wave analysis monthly mean wave spectra of the same months will be derived.

2.2 Doppler wind radiometer

In 2012 the novel wind radiometer WIRA (Rüfenacht et al., 2014) was developed at the Institute of Applied Physics at the University of Bern. It is the only instrument capable of steadily observing wind in the otherwise sparsely probed atmospheric layer between 35 and 70 km altitude. Other techniques like rocket (Schmidlin, 1986) or lidar-based measurements (Lübken et al., 2016; Baumgarten et al., 2015) can provide wind data in this region with a higher vertical and temporal resolution than WIRA but suffer from high operational costs (rockets, lidar) or cloudy conditions (lidar). Meteorological rocket soundings are thus only suitable for short campaigns, not for continuous observations. WIRA, a ground-based passive microwave heterodyne receiver, observes the Doppler shifts of the pressure-broadened emission line of ozone at 142 GHz. The retrieval of zonal and meridional middle-atmospheric wind components is based on OEM. The measurement uncertainty ranges from 10 to 20 m s⁻¹, and the

vertical resolution varies between 10 and 16 km. For more detailed information about the instrument we refer to papers by Rüfenacht et al. (2012, 2014). In order to resolve the 18 h wave, the retrieval was pushed to the limits by using measurements with an integration time of 6 h only, instead of the usual 24 h averages. Therefore, a new retrieval version which improves the wind accuracy of the mesospheric zonal wind estimates has been used in this study. However the data quality of the meridional wind component retrieved from 6 hourly spectral line integrations is mediocre and thus not used in our study. In order to retrieve the meridional wind in the middle atmosphere, a much longer integration time, like 24 h, is needed.

The WIRA instrument was capable of observing a quasi 18 h zonal wind oscillation for the time period between 25 January and 10 February 2013 within the pressure range 0.1–1 hPa. During that time the wind radiometer was deployed at the observatory in Haute-Provence (43.56° N, 5.43° E) within the scope of the ARISE (Atmospheric dynamics Research InfraStructure in Europe) project. Figure 4 shows the uninterrupted zonal wind data set as measured by WIRA between 25 January and 10 February 2013. In the whole altitude domain the measurement response of the WIRA radiometer is greater than 80 %.

3 Numerical method

In order to derive the wave spectrum of the MIAWARA H₂O data time series, we applied the following numerical methods: a digital band-pass filter (non-recursive finite impulse response) with a comprised Hamming window is applied to the data time series to extract amplitudes of hidden oscilla-

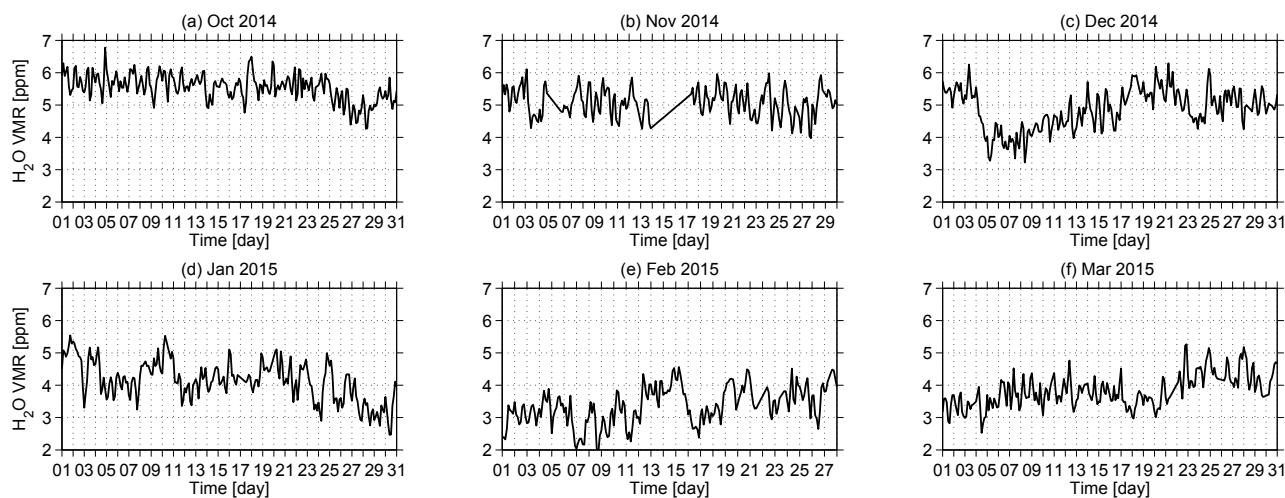


Figure 2. Monthly time series of MIAWARA H₂O (ppm) averaged between 0.02 and 0.1 hPa for winter 2014/2015.

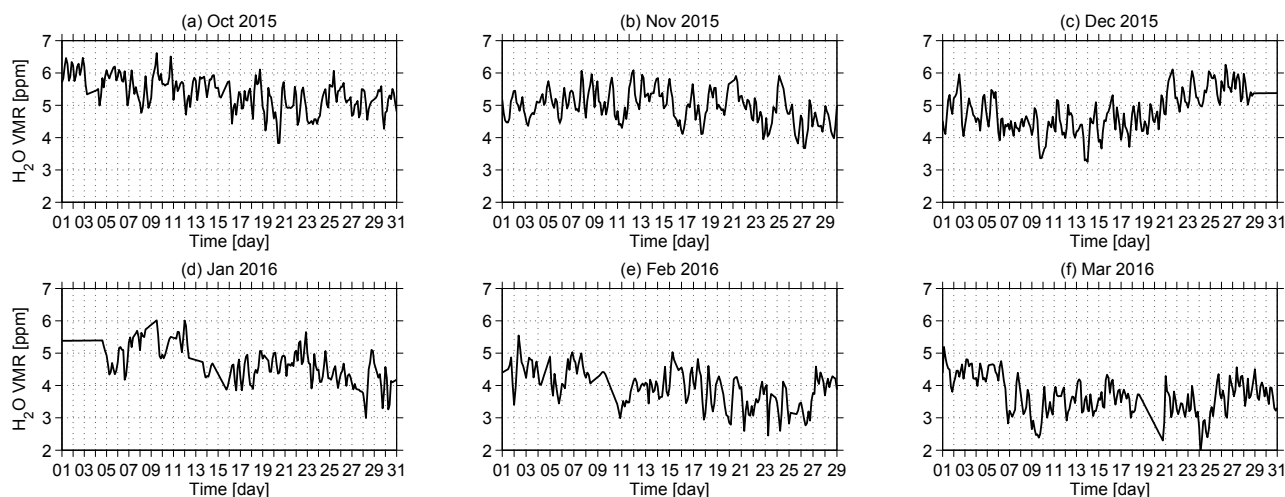


Figure 3. Same as Fig. 2 but for winter 2015/2016.

tions of periods between 6 and 30 h. Performing windowing methods to measurement time series ensures that the data end points fit together and smooths out short-term fluctuations to put longer-term cycles in the foreground. Therefore the spectral leakage can be reduced (Harris, 1978). In Studer et al. (2012) the numerical structure of the band-pass filter was shown. Lately the filter has been used to investigate the impact of the 27-day solar rotation cycle on mesospheric water vapor (Lainer et al., 2016) and to analyze the quasi 16-day planetary wave during boreal winter (Scheiben et al., 2014). We follow the advice from Oppenheim et al. (1989) and run the filter with a zero phase lag forward and backward along the measurement time series. The cutoff frequencies of the band-pass attenuation are set to either 5 or 16.6% (depending on the analysis method) of the initialized central frequency. The central frequency prearranges the size of the Hamming

window, which is triple that of the central period. Our filter and window setup guarantees a fast adaptability to data variations in time.

4 Results

4.1 Monthly mean H₂O wave spectra

A mean wave amplitude is obtained by averaging amplitude series over time. For example, a final H₂O wave amplitude spectrum as presented in Figs. 5 and 6 is created by computing the monthly averaged amplitudes as a function of the period. The period range goes from 6 to 30 h with a spectral resolution of 1 h. Overall, 12 months of microwave radiometric water vapor measurements were processed. The mean amplitude wave spectra reveal that except for Octo-

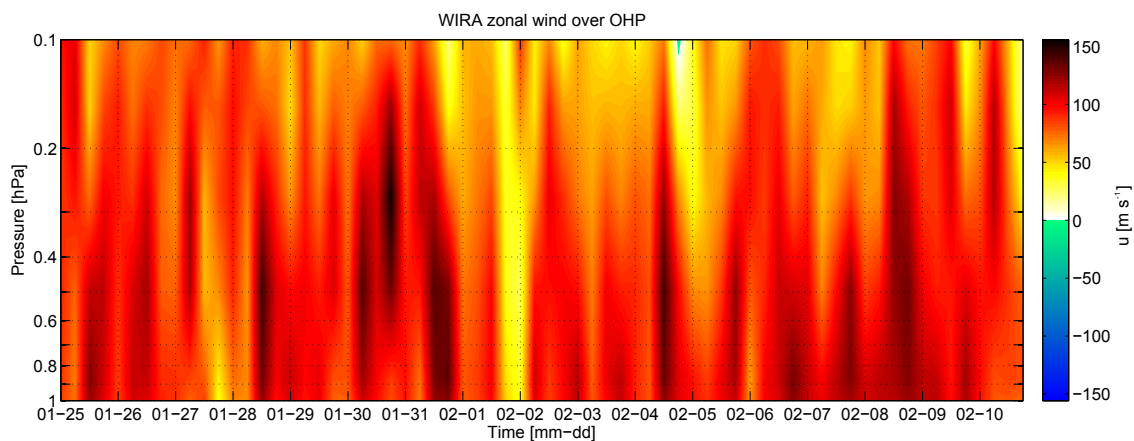


Figure 4. The zonal wind vector component time series (m s^{-1}) measured by WIRA between 25 January and 10 February 2013 in the pressure range 0.1–1 hPa at the Observatoire de Haute-Provence (OHP) in France.

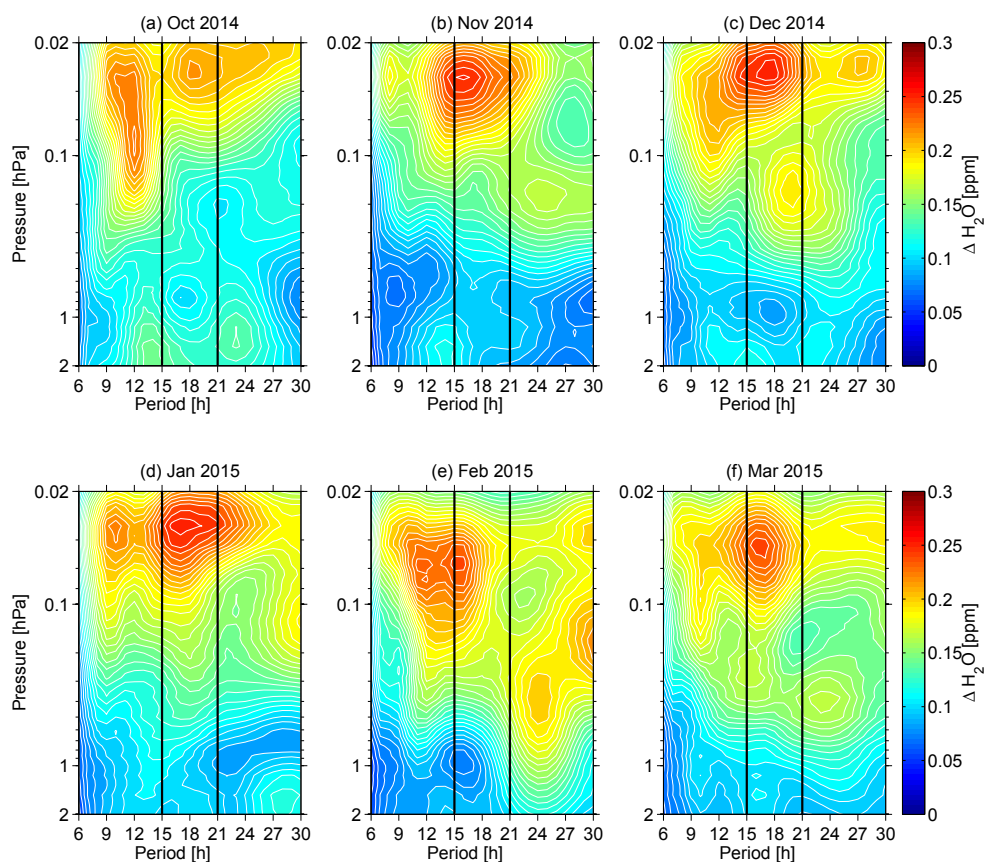


Figure 5. The MIAWARA water vapor monthly mean wave spectrum with periods between 6 and 30 h. Shown is the result of the H₂O amplitudes (ppm) for the months October 2014 to March 2015 (a–f). The border of the quasi 18 h period band (15–21 h) is indicated by the vertical black line pair.

ber 2014 the highest wave amplitudes are located in the 18 h period band for the 2014/15 period. During October 2014 a different regime close to a 12 h period is dominating. Below 1 hPa amplitudes in water vapor are small. Regarding the

18 h variability the altitude domain above 0.1 hPa is most interesting. During the 2015/16 period clear 18 h signals can be found in November 2015 and January and February 2016 (Fig. 6). During the other 3 months (October and December

2015, March 2016) high amplitudes show up with periods near 12 and 24 h (tidal patterns). Clear and high wave amplitudes at exactly 18 h are found in December 2014 (Fig. 5c), January 2016 (Fig. 6d) and February 2016 (Fig. 6e). The altitude region where the 18 h oscillation is prominent is mostly above 0.1 hPa. We find monthly mean quasi 18 h H₂O amplitudes in the range 0.2–0.3 ppm. Prominent wave events with sharp 18 h periods happened in January and February 2016. Within the subsequent section we investigate how often the 18 h wave packets have been observed in the MIAWARA water vapor time series.

4.2 Temporal evolution of quasi 18 h wave

We present the whole temporal evolution (12 months) of the water vapor oscillations in the quasi 18 h period band for MIAWARA. Absolute and relative wave amplitudes, which are calculated relative to the average water vapor mixing ratio at a pressure level over the investigated time period, are presented.

Both the absolute and the relative amplitudes of the 18 h wave in the MIAWARA observations show that this wave occurs quite regularly during the investigated winter months (Figs. 7 and 8). The amplitudes of the wave become highest above the mid-mesosphere (0.1 hPa). Local (in time) amplitudes reach up to 0.5 ppm or 12 % in relative units. Scheiben et al. (2013) showed that in the altitude range from 3 to 0.05 hPa the diurnal H₂O amplitudes do not exceed 0.05 ppm. The 18 h H₂O wave emerges in packets, and a growing of the amplitudes with decreasing pressure can be identified. Both wave characteristics could be reminiscent of inertia-gravity waves. But since the 18 h period exceeds the inertia period for the location of Bern by about 1.5 h, some background wind speed is required that adjusts a lower intrinsic wave period to the 18 h period observed from ground via Doppler shifting.

From 20 November 2012 to 6 May 2013 WIRA observed middle-atmospheric wind from the Observatoire de Haute-Provence within the district of Alpes-de-Haute-Provence in southern France. A continuous phase of 6-hourly resolved observations for about 17 days makes it possible to search for 18 h wave activity, and strong zonal wind 18 h wave components could be identified (Fig. 9). A comparison of zonal wind and water vapor wave amplitudes could be misleading since the latter highly depends on the vertical gradient. Thus such a comparison is not performed and the zonal wind analysis shown here has to be seen as an independent result and short part of the paper.

The temporal distribution of the absolute zonal wind amplitudes is shown in Fig. 9a. During the observation period the quasi 18 h waves show no preference for certain altitudes and emerge at very different pressure levels. On 10 February 2013 the highest wave amplitudes appear between 0.1 and 0.2 hPa and reach 30–35 m s⁻¹, which is about 50 % (Fig. 9b) of the mean wind speed over the 17 investigated days at these

pressure levels. A second, bigger wave event is located at lower altitudes (below 0.5 hPa) and takes place between 31 January and 3 February 2013. But the relative wave amplitudes do not exceed around 30 %. The appearance of these wave events is occasional, and they last for a few 18 h cycles, but not for a longer period. Qualitatively, this looks like the same behavior as revealed by the water vapor analysis. A rough estimate of the pressure-layer-averaged (0.1–1 hPa) RMSEs (root mean square errors) of the absolute zonal wind wave amplitudes have values between 3.3 and 6.6 m s⁻¹ over the investigated time period. The temporal mean RMSE of the zonal wind amplitudes is 5.4 m s⁻¹. After measuring the signal power of the WIRA zonal wind time series, white Gaussian noise was added to reach a signal-to-noise ratio of 5 dB. The RMSE then was calculated from two spectral filter analyses of the noisy and original data set.

In the first part of Sect. 4.3 we will expand on possible MIAWARA instrument and retrieval artifacts that might have an influence on our data variability in the sub-diurnal time period. In conclusion we clarify that the observed oscillations are robust. Later we discuss the results given in Sect. 4 in the context of other performed studies related to inertia-gravity wave activity and nonlinear wave–wave interactions in the winter midlatitude middle atmosphere.

4.3 Discussion

A spectral analysis of local instrument-related temperatures at the MIAWARA measurement site – such as outdoor temperatures, indoor temperatures, mixer temperatures, Aquiris FFT FPGA (Field Programmable Gate Array) temperatures, hot-load temperatures and receiver temperatures – has been performed to see whether similar prominent 18 h oscillations are present with a possible influence on the observed wave signatures in the H₂O retrieval data. The individual temperature amplitudes were examined for several months. Figure 10 shows the monthly mean temperature amplitudes for the six different parameters in January, February and March 2016. As illustrated in Fig. 6 high wave activity with periods between 15 and 21 h was seen in January and February 2016 but not in March 2016. Local peaks in the monthly mean amplitude spectra occur close to 24 and 12 h for T_{Outdoor} , T_{Indoor} , T_{Mixer} , T_{FPGA} and T_{Hot} , representing the diurnal temperature cycle. A typical value for the receiver temperature T_{Rec} , which is a parameter for the internally generated noise power of the MIAWARA receiver, is on the order of 160 K, and the monthly average amplitude variability between the investigated periods is below 2 K. No distinct and strong variability can be identified in the period range between 15 and 21 h for all temperature parameters that might effect the measured H₂O line spectrum at 22.235 GHz. The atmospheric temperature profile that is used in the retrieval calculation as a forward-model parameter is a 3-day average profile calculated from Aura MLS observations and thus cannot generate any regular perturbations at 18 h time intervals to our

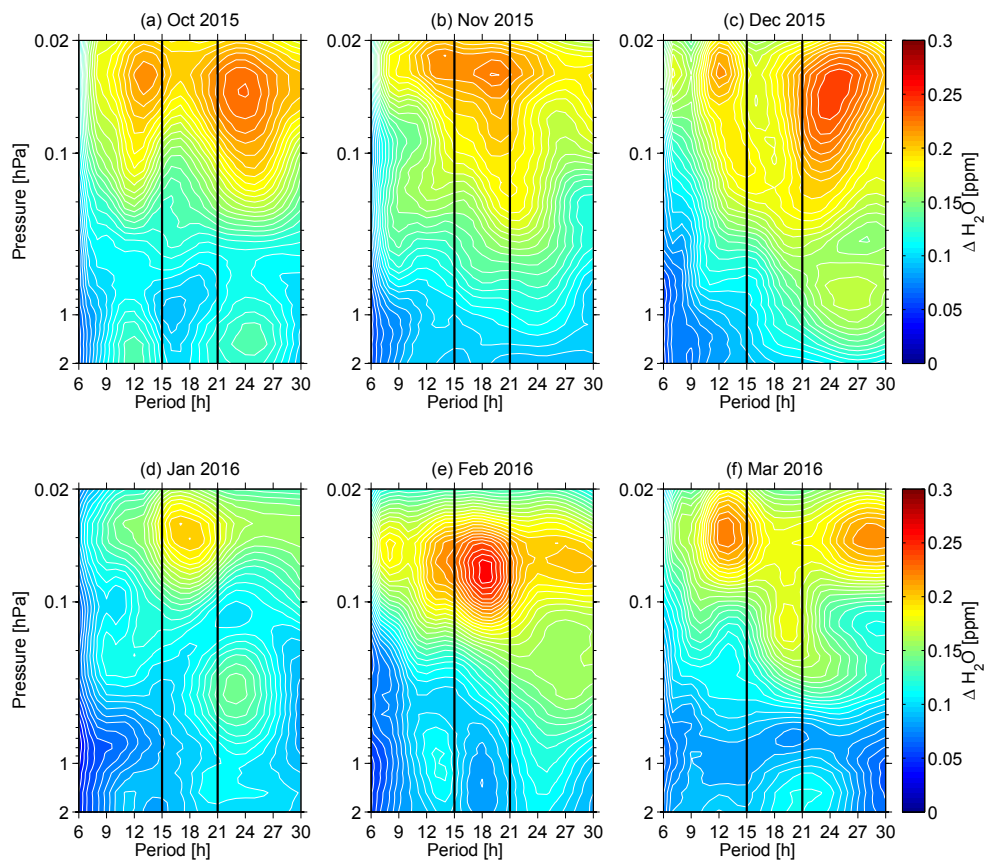


Figure 6. Same as Fig. 5 but for the months October 2015 to March 2016 (a–f).

retrievals. Another parameter that is needed for the calibration of the H₂O radiometer is the cold-sky brightness temperature, which is dependent on the opacity. The atmospheric opacity at 22.235 GHz is obtained from a tipping curve iteration according to Han and Westwater (2000) and was also analyzed for oscillations, but only semi-diurnal and diurnal variations were found, which is not unusual and related to changes in tropospheric humidity. Further, we use a monthly mean zonal mean water vapor climatology based on Aura MLS v2.2 measurements between 2004 and 2010 as a priori information in the retrieval process, which is not expected to influence the observed H₂O oscillations. Although the a priori itself only varies monthly, the measurement response as shown by the white horizontal lines in Fig. 1 varies on a much shorter timescale. This is due to the fact that the a priori contribution, which is the sensitivity of the retrieval to the a priori profile, depends on the actual smoothing error related to a single H₂O profile retrieval with the integrated (in our case 3 h) microwave line spectrum. To our knowledge it is not known how and if any short-term variability of the measurement response affects the amount of retrieved water vapor. To clarify the terms a priori contribution (A_c)

and measurement response (M_r), the conversion equation of these two quantities is given:

$$A_c = 100\% - M_r. \quad (1)$$

A spectral analysis of the a priori contribution in the MIAWARA data over the whole altitude range of the radiometer (0.01–10 hPa) was performed. In total we show here 3 months in the beginning of the year 2016 (Fig. 11). All 3 months have mean wave amplitudes below 7% at pressure levels above 0.1 hPa, but the peaks are clearly outside of the quasi 18 h period band.

Many parameter tests were performed to see whether a similar 18 h variability could contaminate the data retrieval of the MIAWARA instrument and lead to artificial effects. This can be excluded, and therefore the observed oscillations in water vapor are expected to be a real atmospheric feature. Since the focus of the paper is on water vapor, we will not expand the parameter tests on the wind retrieval here. Next, a short review on possible explanations for the quasi 18 h wave will be given.

As mentioned in Li et al. (2007), the 18 h oscillation in mesospheric water vapor could be connected to the presence of low-frequency gravity waves (GWs), also called inertia-

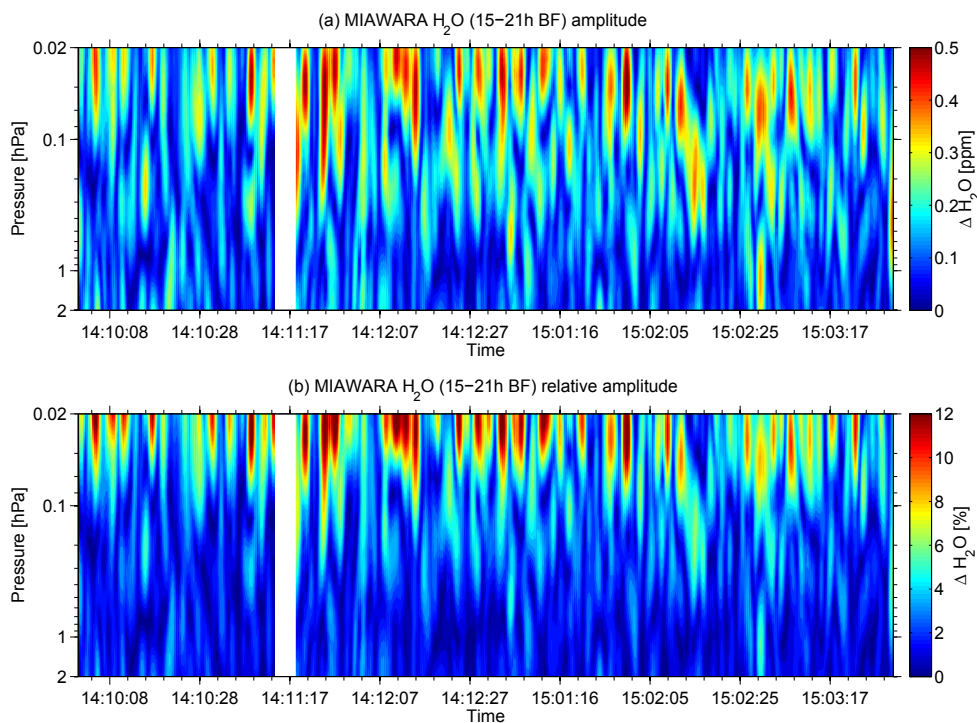


Figure 7. Temporal evolution of wave amplitudes derived from band-pass Hamming-window-filtered MIAWARA H₂O volume mixing ratio time series with cutoff periods at 15 and 21 h. Shown is the time period from October 2014 to March 2015.

gravity waves, of a similar apparent period. In general, gravity waves are a natural feature of a stably stratified atmosphere, where the squared Brunt–Väisälä frequency $N^2 > 0$. Gravity waves can be classified into three types, with low, medium or high intrinsic wave angular frequencies $\hat{\omega}$ (Fritts and Alexander, 2003). The role of atmospheric gravity waves is to transport and deposit momentum by wave-breaking. Besides shear instability, GW breaking events are an important source of turbulent kinetic energy production near the mesopause (Fritts et al., 2003). As the sub-spectrum of gravity waves is large, plenty of different triggering mechanisms exist, including: orographic lifting, spontaneous emission from jet streams and fronts, convective systems and water waves on oceans. Strong emissions of atmospheric gravity waves of low frequency (periods from a few hours to about 24 h) were detected in the exit region of jets in the upper troposphere, as presented by Plougonven and Zhang (2014) and references therein. A coherent 10.5 h low-frequency GW packet with vertical wavelengths between 4 and 10 km has been studied by Nicolls et al. (2010). They suggest a geostrophic adjustment of the tropospheric jet stream a few days before the actual observation as the main triggering mechanism of the inertia-gravity wave packet.

Li et al. (2007) described an 18 h inertia-gravity wave. They used sodium-lidar measurements to probe the atmosphere between 80 and 110 km. In a campaign lasting 80 h (December 2004), observations of temperature, sodium den-

sity, zonal and meridional wind were conducted. A linear least-squares data fitting revealed strong amplitudes in the wind fields with a characteristic increase with altitude. Wind amplitude peaks were detected between 96 and 101 km. The 18 h signal was also present in temperature and sodium density, albeit less distinct. By applying linear wave theory (for details see, e.g., Chapter 2 in Nappo, 2002), an estimation of the horizontal wave propagation direction (245°), wavelength (about 1800 km) and phase speed (28 m s^{-1}) could be determined for the first time with experimental data from a single instrument (Li et al., 2007). The vertical wavelengths were estimated to be between 15 and 18 km below an altitude of 97 km. The upper measurement limit of the MIAWARA water vapor radiometer is approximately at an altitude of 75 km (0.02 hPa) and does not reach the same altitudes as the previously mentioned sodium-lidar system. Still the vertical resolution of our instruments would be high enough to capture inertia-gravity waves with vertical wavelengths of about 20 km or larger. An advantage of microwave radiometers is that they can measure during day and night in a continuous operating mode and are not critically influenced by the occurrence of clouds, whereas lidar instruments usually are.

Revealing the possible observation of an 18 h inertia-gravity wave in our measurements would require more co-located atmospheric profile measurements of both zonal and meridional wind and temperature. The main point would be to check if the vertical wavelengths are large enough to be

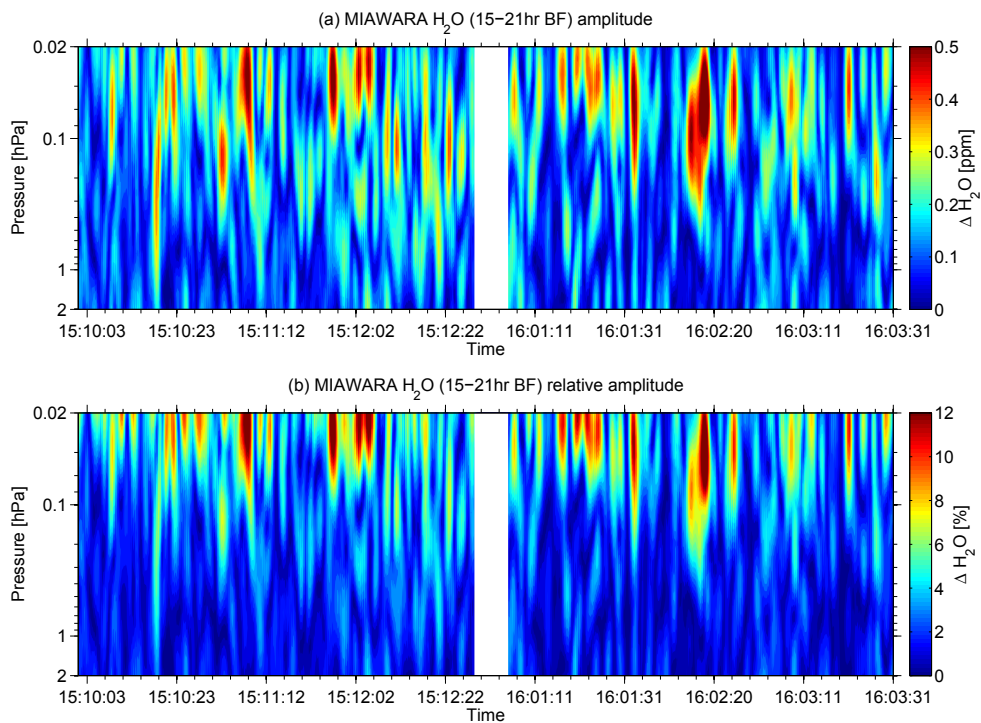


Figure 8. Same as Fig. 7, but here the time period from October 2015 to March 2016 is shown. The measurement gap between 28 December 2015 and 4 January 2016 is indicated by the white bar.

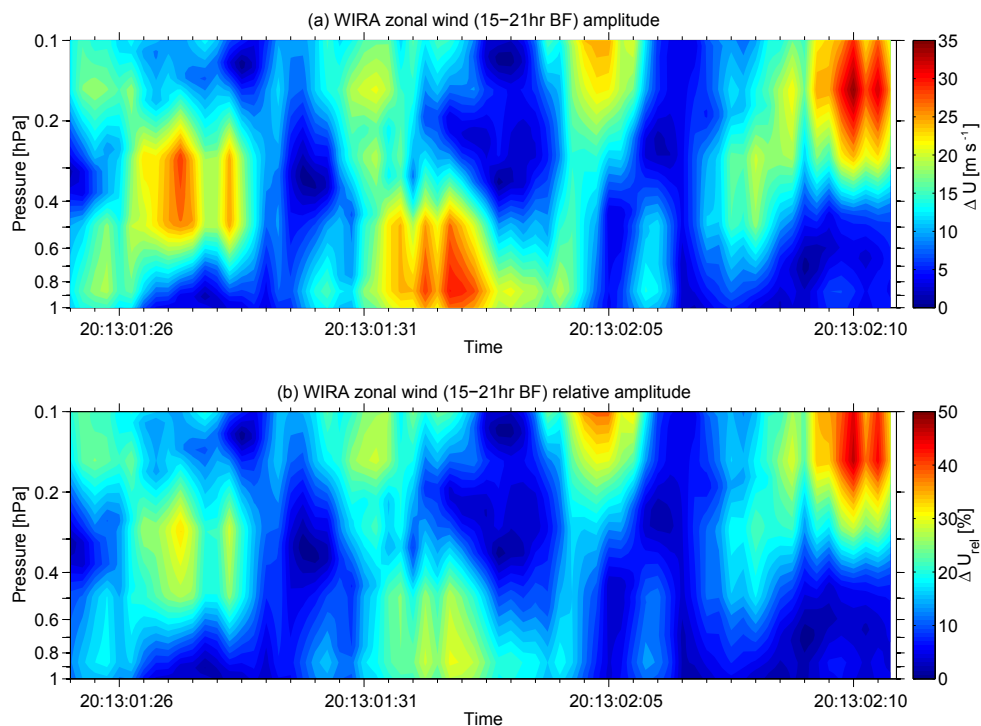


Figure 9. WIRA zonal wind band-pass-filtered (15–21 h) absolute (a) and relative (b) wave amplitudes in the pressure range 0.1–1 hPa between 25 January and 10 February 2013.

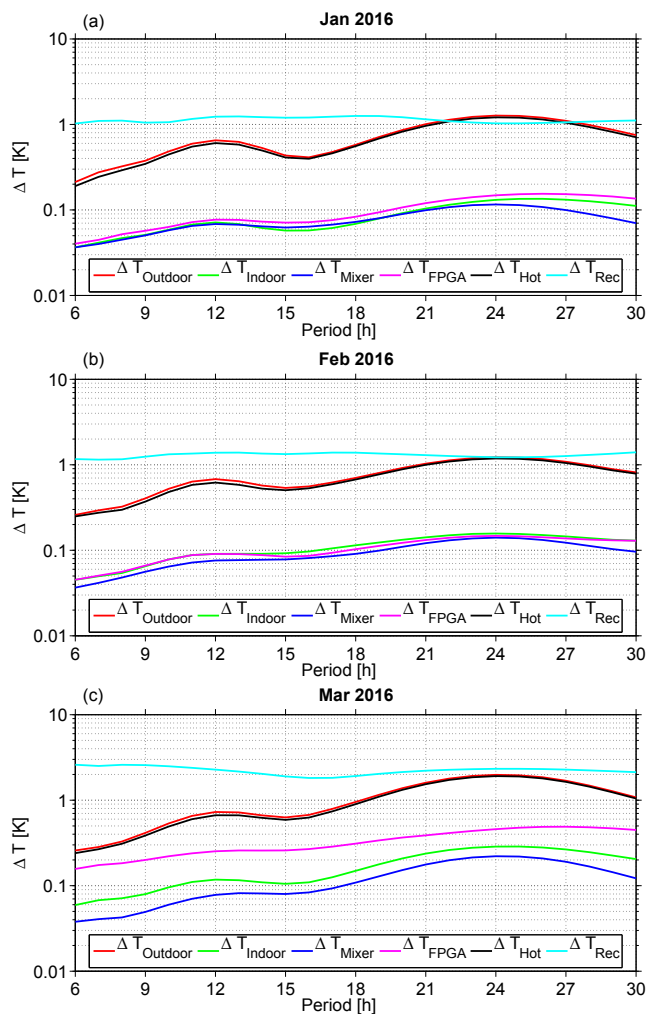


Figure 10. Monthly mean spectral wave analysis for six different temperature parameters related to the MIAWARA water vapor radiometer: outdoor, indoor, mixer, FPGA, hot-load and receiver temperature. Spectral analysis goes from 6 to 30 h with a resolution of 1 h. The results are shown for January, February and March 2016.

detectable for our microwave radiometric observations with a finest vertical resolution of 10 km. Further, in the case of inertia-gravity waves with a ground-related frequency of around 18 h a specific background wind speed is required that reduces the actual intrinsic wave frequency (Doppler shifting) below the period of 16.44 h corresponding to the inertia frequency at the latitude of Bern.

In principle it would be possible to apply the hodograph method (Sawyer, 1961) with wind data from the WIRA radiometer and derive inertia-gravity wave parameters. During the time period when the WIRA data were analyzed for this study the instrument was not able to provide meridional winds in the temporal resolution required. Thus we were not able to derive hodographs in the upper mesosphere. We note that a substantial number of gravity wave studies (Li et al.,

2007; Plougonven and Teitelbaum, 2003; Baumgarten et al., 2015) have made use of the hodograph analysis.

A Doppler wind and temperature lidar measurement campaign in northern Norway by Baumgarten et al. (2015) identified a number of inertia-gravity wave cases at altitudes between 60 and 70 km with emphasis on upward propagation and vertical wavelengths in the range 5–10 km. One observed gravity wave had an apparent period of approximately 11 h. Such a gravity wave could not be observed with our microwave radiometers due to a too-low vertical resolution.

Another complication in the comparison between wind and H₂O wave signatures comes from oscillations in H₂O that may be caused by the polar vortex edge moving across the observation site. Across the polar vortex edge large meridional gradients in H₂O tracer concentrations exist. A regular movement of the whole vortex could therefore trigger oscillations in atmospheric H₂O profile measurements. Indeed we find such oscillations of the polar vortex edge during winter above Bern, but the dominant period is 24 h in the mesosphere (0.01–1 hPa). We could not find any connection to an 18 h period, which we are focusing on in this study.

Besides the potential observation of inertia-gravity wave activity in our presented H₂O and zonal wind data sets, there seems to be another possibility of a nonlinear wave coupling between a 2-day wave and the diurnal tide. Lieberman et al. (2017) use the global NOGAPS (Navy Operational Global Atmospheric Prediction System) ALPHA (Advanced Level Physics High Altitude) model to investigate a nonlinear interaction between the migrating diurnal tide and the westward-propagating quasi 2-day wave. This interaction results in a westward-traveling wave component (W4) of zonal wave number 4 with an apparent period of 16 h and an eastward-propagating wave of zonal wave number 2 with a period of 2 days. Amplitudes of W4 are largest in the midlatitude winter mesosphere, and the wind magnitudes in the MLT typically reach 10 m s⁻¹ in the model data. However wind amplitudes from meteor radar measurements at Bear Lake (42° N, 111.3° W) exceeded those from the NOGAPS ALPHA model system. The maximal zonal wind amplitudes of the 18 h wave component observed by WIRA at a comparable latitude reach about 30–35 m s⁻¹ in the mid-mesosphere. But the lower altitude of the WIRA measurements impedes an acceptable comparison to results in the paper of Lieberman et al. (2017).

Given the fact that the W4 wave shows inertia-gravity-wave-like features and has a period within our defined quasi 18 h period band, it is likely that we observed such a described W4 wave in our spectral data analyses. For November 2014 and February and March 2015 the monthly mean amplitude peaks in the water vapor wave spectrum is closer to 16 than to 18 h, which could be a clue for a W4 wave. In contrast to satellite observations, the temporal resolution of the local profile measurements, which our instruments provide, are not outside the Nyquist limits of temporal resolution for the westward-traveling 16 h W4 wave. The information of

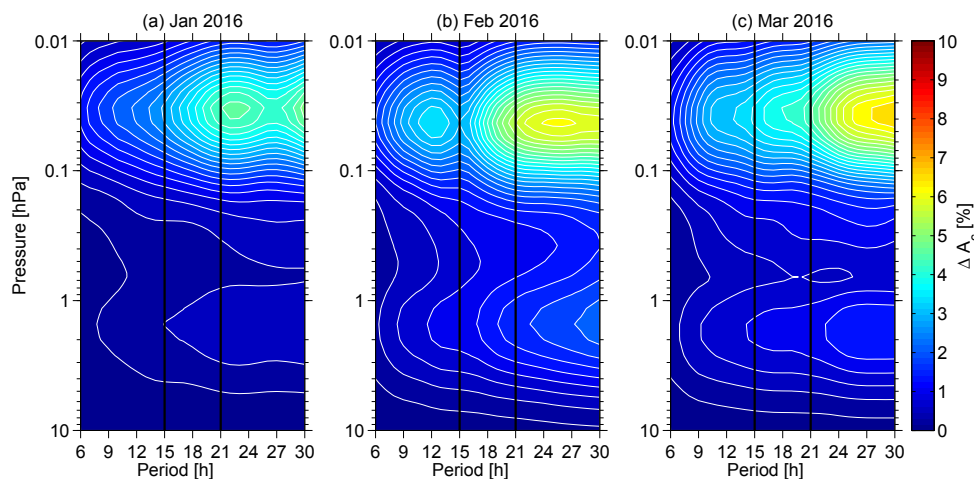


Figure 11. Spectral analysis of the a priori contribution in the MIAWARA water vapor retrievals for periods between 6 and 30 h. Shown are monthly mean absolute wave amplitudes of the a priori contribution ΔA_c (in %) for January (a), February (b) and March (c) 2016.

long-term microwave radiometric observations of nonlinear wave–wave couplings such as W4 could be very useful for validating numerical model results.

5 Conclusions

For the first time a dominant quasi 18 h wave in mesospheric water vapor has been reported from ground-based measurements. A unique data set from the MIAWARA instrument with a temporal resolution of 3 h has been examined for wave signatures with periods between 6 and 30 h. Two winter time periods were used to present monthly mean wave spectra of H₂O. For a considerable number of months prominent wave signatures in the quasi 18 h (15–21 h) period band have been identified. The packet-like occurrence in time and growing amplitudes with decreasing pressure are an inertia-gravity-wave-like feature.

In the first part of Sect. 4.3 we clarified that our ground-based observations are robust and that the retrievals are not contaminated by any considerable artifacts. Whether the observed wave is a direct image of a low-frequency inertia-gravity wave is not definitely clear, but gravity waves with comparable frequencies have been observed at mesospheric altitudes in the winter hemisphere. Another promising clarification approach is the mentioned nonlinear coupling of the quasi 2-day wave to the migrating diurnal tide. A much more detailed analysis of the quasi 2-day wave behavior above Bern is necessary to understand the complex interactions and wave couplings we identified in mesospheric water vapor and zonal wind profile time series. This is an encouraging future research project.

It has been shown that the Doppler wind radiometer WIRA is capable of resolving sub-diurnal oscillations in the zonal wind component. The quality of the meridional wind mea-

surements has potential for improvement and could contribute to wave characteristic analyses in the near future. Quasi 18 h oscillations were detected in the WIRA zonal wind data set for a period of about 17 days. There are also meteor-radar-based measurements (Huang et al., 2013), where similar wave periods (~ 16 h) are observed. At the very least the different wind observations could provide an additional constraint for three-dimensional model simulation studies achievable with for instance WACCM (Whole Atmosphere Community Climate Model) or ECHAM. A useful exercise could aim at validating the correct representation of nonlinear wave–wave couplings in different models involving tides and planetary waves like the quasi 2-day wave.

Data availability. Data from the ground-based microwave radiometer MIAWARA are publicly available from the NDACC database as monthly files with a diurnal temporal resolution (<ftp://ftp.cpc.ncep.noaa.gov/ndacc/station/bern>). MIAWARA data with a higher temporal resolution and the wind data from WIRA presented in this paper can be made available on request.

Author contributions. ML was responsible for the ground-based water vapor measurements, performed the data analysis and prepared the manuscript. KH designed the filter algorithm and contributed to the interpretation of the results. RR is in charge of WIRA, the ground-based wind radiometer, and provided wind retrieval data. NK is the lead of the project group. All authors read and approved the current version of the manuscript.

Competing interests. The authors declare that they have no conflict of interest.

Acknowledgements. This work is supported by Swiss National Science Foundation grant 200020-160048 and MeteoSwiss in the frame of the GAW project “Fundamental GAW parameters measured by microwave radiometry”. Rolf Rüfenacht is supported by post-doc grant P2PEB2-165383. The authors acknowledge NASA for access to Aura MLS data and are grateful for constructive comments provided during the review process.

Edited by: Gabriele Stiller

Reviewed by: four anonymous referees

References

- Baumgarten, G., Fiedler, J., Hildebrand, J., and Lübken, F.-J.: Inertia gravity wave in the stratosphere and mesosphere observed by Doppler wind and temperature lidar, *Geophys. Res. Lett.*, 42, 10929–10936, <https://doi.org/10.1002/2015GL066991>, 2015.
- Belova, A., Kirkwood, S., Murtagh, D., Mitchell, N., Singer, W., and Hocking, W.: Five-day planetary waves in the middle atmosphere from Odin satellite data and ground-based instruments in Northern Hemisphere summer 2003, 2004, 2005 and 2007, *Ann. Geophys.*, 26, 3557–3570, <https://doi.org/10.5194/angeo-26-3557-2008>, 2008.
- Brasseur, G. and Solomon, S.: *Aeronomy of the Middle Atmosphere: Chemistry and Physics of the Stratosphere and Mesosphere*, Vol. 32, Springer, 2006.
- Deuber, B., Kämpfer, N., and Feist, D. G.: A new 22-GHz Radiometer for Middle Atmospheric Water Vapour Profile Measurements, *IEEE T. Geosci. Remote*, 42, 974–984, <https://doi.org/10.1109/TGRS.2004.825581>, 2004.
- Deuber, B., Haeefe, A., Feist, D. G., Martin, L., Kämpfer, N., Nedoluha, G. E., Yushkov, V., Khaykin, S., Kivi, R., and Vomel, H.: Middle Atmospheric Water Vapour Radiometer – MIAWARA: Validation and first results of the LAUTLOS/WAVVAP campaign, *J. Geophys. Res.*, 110, D13306, <https://doi.org/10.1029/2004JD005543>, 2005.
- Eriksson, P., Jiménez, C., and Buehler, S. A.: Qpack, a general tool for instrument simulation and retrieval work, *J. Quant. Spectrosc. Ra.*, 91, 47–64, <https://doi.org/10.1016/j.jqsrt.2004.05.050>, 2005.
- Eriksson, P., Buehler, S., Davis, C., Emde, C., and Lemke, O.: ARTS, the atmospheric radiative transfer simulator, version 2, *J. Quant. Spectrosc. Ra.*, 112, 1551–1558, <https://doi.org/10.1016/j.jqsrt.2011.03.001>, 2011.
- Forbes, J. M.: Vertical coupling by the semidiurnal tide in Earth’s atmosphere, in: *Climate and Weather of the Sun-Earth System (CAWSES): Selected Papers from the 2007 Kyoto Symposium*, edited by: Tsuda, T., Fujii, R., Shibata, K., and Geller, M. A., TERRAPUB, Tokyo, 337–348, 2009.
- Forbes, J. M., Hagan, M. E., Miyahara, S., Vial, F., Manson, A. H., Meek, C. E., and Portnyagin, Y. I.: Quasi 16-day oscillation in the mesosphere and lower thermosphere, *J. Geophys. Res.-Atmos.*, 100, 9149–9163, <https://doi.org/10.1029/94JD02157>, 1995.
- Fritts, D. C. and Alexander, M. J.: Gravity wave dynamics and effects in the middle atmosphere, *Rev. Geophys.*, 41, 1003, <https://doi.org/10.1029/2001RG000106>, 2003.
- Fritts, D. C., Bizon, C., Werne, J. A., and Meyer, C. K.: Layering accompanying turbulence generation due to shear instability and gravity-wave breaking, *J. Geophys. Res.-Atmos.*, 108, 8452, <https://doi.org/10.1029/2002JD002406>, 2003.
- Hagan, M. E. and Forbes, J. M.: Migrating and nonmigrating diurnal tides in the middle and upper atmosphere excited by tropospheric latent heat release, *J. Geophys. Res.-Atmos.*, 107, ACL 6-1–ACL 6-15, <https://doi.org/10.1029/2001JD001236>, 2002.
- Han, Y. and Westwater, E. R.: Analysis and improvement of tipping calibration for ground-based microwave radiometers, *IEEE T. Geosci. Remote*, 38, 1260–1276, <https://doi.org/10.1109/36.843018>, 2000.
- Hardiman, S. C., Butchart, N., Charlton-Perez, A. J., Shaw, T. A., Akiyoshi, H., Baumgaertner, A., Bekki, S., Braesicke, P., Chipperfield, M., Dameris, M., Garcia, R. R., Michou, M., Pawson, S., Rozanov, E., and Shibata, K.: Improved predictability of the troposphere using stratospheric final warmings, *J. Geophys. Res.-Atmos.*, 116, D18113, <https://doi.org/10.1029/2011JD015914>, 2011.
- Harris, F. J.: On the use of windows for harmonic analysis with the discrete Fourier transform, *Proc. IEEE*, 66, 51–83, <https://doi.org/10.1109/PROC.1978.10837>, 1978.
- Huang, K. M., Liu, A. Z., Lu, X., Li, Z., Gan, Q., Gong, Y., Huang, C. M., Yi, F., and Zhang, S. D.: Nonlinear coupling between quasi 2 day wave and tides based on meteo radar observations at Mauri, *J. Geophys. Res.- Atmos.*, 118, 10936–10943, <https://doi.org/10.1002/jgrd.50872>, 2013.
- Jacobi, C., Schindler, R., and Kürschner, D.: Planetary wave activity obtained from long-period (2–18 days) variations of mesopause region winds over Central Europe (52° N, 15° E), *J. Atmos. Sol.-Terr. Phys.*, 60, 81–93, [https://doi.org/10.1016/S1364-6826\(97\)00117-X](https://doi.org/10.1016/S1364-6826(97)00117-X), 1998.
- Kämpfer, N., Nedoluha, G., Haeefe, A., and De Wachter, E.: *Microwave Radiometry*, Vol. 10 of ISSI Scientific Report Series, Springer New York, <https://doi.org/10.1007/978-1-4614-3909-7>, 2012.
- Lainer, M., Kämpfer, N., Tschanz, B., Nedoluha, G. E., Ka, S., and Oh, J. J.: Trajectory mapping of middle atmospheric water vapor by a mini network of NDACC instruments, *Atmos. Chem. Phys.*, 15, 9711–9730, <https://doi.org/10.5194/acp-15-9711-2015>, 2015.
- Lainer, M., Hocke, K., and Kämpfer, N.: Variability of mesospheric water vapor above Bern in relation to the 27-day solar rotation cycle, *J. Atmos. Sol.-Terr. Phys.*, 143–144, 71–87, <https://doi.org/10.1016/j.jastp.2016.03.008>, 2016.
- Li, T., She, C.-Y., Liu, H.-L., Leblanc, T., and McDermid, I. S.: Sodium lidar-observed strong inertia-gravity wave activities in the mesopause region over Fort Collins, Colorado (41° N, 105° W), *J. Geophys. Res.-Atmos.*, 112, D22104, <https://doi.org/10.1029/2007JD008681>, 2007.
- Lieberman, R. S., Riggan, D. M., Nguyen, V., Palo, S. E., Siskind, D. E., Mitchell, N. J., Stober, G., Wilhelm, S., and Livesey, N. J.: Global observations of 2 day wave coupling to the diurnal tide in a high-altitude forecast-assimilation system, *J. Geophys. Res.-Atmos.*, 122, 4135–4149, <https://doi.org/10.1002/2016JD025144>, 2017.
- Liu, J., Tarasick, D. W., Fioletov, V. E., McLinden, C., Zhao, T., Gong, S., Sioris, C., Jin, J. J., Liu, G., and Moeini, O.: A global ozone climatology from ozone soundings via trajectory mapping: a stratospheric perspective, *Atmos. Chem. Phys.*, 13, 11441–11464, <https://doi.org/10.5194/acp-13-11441-2013>, 2013.

- Livesey, N. J., Read, W. G., Wagner, P. A., Froidevaux, L., Lambert, A., Manney, G. L., Millán Valle, L. F., Pumphrey, H. C., Santee, M. L., Schwartz, M. J., Wang, S., Fuller, R. A., Jarnot, R. F., Knosp, B. W., and Martinez, E.: Version 4.2x Level 2 data quality and description document, Tech. rep., Jet Propulsion Laboratory, California Institute of Technology, 2015.
- Lübken, F.-J., Baumgarten, G., Hildebrand, J., and Schmidlin, F. J.: Simultaneous and co-located wind measurements in the middle atmosphere by lidar and rocket-borne techniques, *Atmos. Meas. Tech.*, 9, 3911–3919, <https://doi.org/10.5194/amt-9-3911-2016>, 2016.
- McDonald, A. J., Hibbins, R. E., and Jarvis, M. J.: Properties of the quasi 16 day wave derived from EOS MLS observations, *J. Geophys. Res.-Atmos.*, 116, D06112, <https://doi.org/10.1029/2010JD014719>, 2011.
- Nappo, C. J.: An introduction to atmospheric gravity waves, Academic Press, 2002.
- Nicolls, M. J., Varney, R. H., Vadas, S. L., Stamus, P. A., Heinselmann, C. J., Cosgrove, R. B., and Kelley, M. C.: Influence of an inertia-gravity wave on mesospheric dynamics: A case study with the Poker Flat Incoherent Scatter Radar, *J. Geophys. Res.-Atmos.*, 115, D00N02, <https://doi.org/10.1029/2010JD014042>, 2010.
- Oppenheim, A. V., Schafer, R. W., and Buck, J. R.: Discrete-time signal processing, Vol. 2, Prentice-hall Englewood Cliffs, 1989.
- Orr, A., Bechtold, P., Scinocca, J., Ern, M., and Janiskova, M.: Improved Middle Atmosphere Climate and Forecasts in the ECMWF Model through a Nonorographic Gravity Wave Drag Parameterization, *J. Climate*, 23, 5905–5926, <https://doi.org/10.1175/2010JCLI3490.1>, 2010.
- Plougonven, R. and Teitelbaum, H.: Comparison of a large-scale inertia-gravity wave as seen in the ECMWF analyses and from radiosondes, *Geophys. Res. Lett.*, 30, 1954, <https://doi.org/10.1029/2003GL017716>, 2003.
- Plougonven, R. and Zhang, F.: Internal gravity waves from atmospheric jets and fronts, *Rev. Geophys.*, 52, 33–76, <https://doi.org/10.1002/2012RG000419>, 2014.
- Riggin, D. M., Liu, H.-L., Lieberman, R. S., Roble III, R. G., J. M. R., Mertens, C. J., Mlynczak, M. G., Pancheva, D., Franke, S. J., Murayama, Y., Manson, A. H., Meek, C. E., and Vincent, R. A.: Observations of the 5-day wave in the mesosphere and lower thermosphere, *J. Atmos. Sol.-Terr. Phys.*, 68, 323–339, <https://doi.org/10.1016/j.jastp.2005.05.010>, 2006.
- Rodgers, C. D.: Inverse methods for atmospheric sounding: theory and practice, Vol. 2, World Scientific Publishing Co Pte. Ltd., 2000.
- Rodgers, C. D. and Prata, A. J.: Evidence for a traveling two-day wave in the middle atmosphere, *J. Geophys. Res.-Oceans*, 86, 9661–9664, <https://doi.org/10.1029/JC086iC10p09661>, 1981.
- Rosenlof, K. H. and Thomas, R. J.: Five-day mesospheric waves observed in Solar Mesosphere Explorer ozone, *J. Geophys. Res.-Atmos.*, 95, 895–899, <https://doi.org/10.1029/JD095iD01p00895>, 1990.
- Rüfenacht, R., Kämpfer, N., and Murk, A.: First middle-atmospheric zonal wind profile measurements with a new ground-based microwave Doppler-spectro-radiometer, *Atmos. Meas. Tech.*, 5, 2647–2659, <https://doi.org/10.5194/amt-5-2647-2012>, 2012.
- Rüfenacht, R., Murk, A., Kämpfer, N., Eriksson, P., and Buehler, S. A.: Middle-atmospheric zonal and meridional wind profiles from polar, tropical and midlatitudes with the ground-based microwave Doppler wind radiometer WIRA, *Atmos. Meas. Tech.*, 7, 4491–4505, <https://doi.org/10.5194/amt-7-4491-2014>, 2014.
- Rüfenacht, R., Hocke, K., and Kämpfer, N.: First continuous ground-based observations of long period oscillations in the vertically resolved wind field of the stratosphere and mesosphere, *Atmos. Chem. Phys.*, 16, 4915–4925, <https://doi.org/10.5194/acp-16-4915-2016>, 2016.
- Salby, M. L.: The 2-day wave in the middle atmosphere: Observations and theory, *J. Geophys. Res.-Oceans*, 86, 9654–9660, <https://doi.org/10.1029/JC086iC10p09654>, 1981a.
- Salby, M. L.: Rossby Normal Modes in Nonuniform Background Configurations. Part I: Simple Fields, *J. Atmos. Sci.*, 38, 1803–1826, [https://doi.org/10.1175/1520-0469\(1981\)038<1803:RNMINB>2.0.CO;2](https://doi.org/10.1175/1520-0469(1981)038<1803:RNMINB>2.0.CO;2), 1981b.
- Sawyer, J. S.: Quasi-periodic wind variations with height in the lower stratosphere, *Q. J. Roy. Meteorol. Soc.*, 87, 24–33, <https://doi.org/10.1002/qj.49708737104>, 1961.
- Scheiben, D., Schanz, A., Tschanz, B., and Kämpfer, N.: Diurnal variations in middle-atmospheric water vapor by ground-based microwave radiometry, *Atmos. Chem. Phys.*, 13, 6877–6886, <https://doi.org/10.5194/acp-13-6877-2013>, 2013.
- Scheiben, D., Tschanz, B., Hocke, K., Kämpfer, N., Ka, S., and Oh, J. J.: The quasi 16-day wave in mesospheric water vapor during boreal winter 2011/2012, *Atmos. Chem. Phys.*, 14, 6511–6522, <https://doi.org/10.5194/acp-14-6511-2014>, 2014.
- Schmidlin, F. J.: Rocket techniques used to measure the neutral atmosphere, Middle Atmosphere Program, Handbook for MAP, 19, R. A. Goldberg, SCOSTEP Secretariat, Univ. of Ill., Urbana, 1–33, 1986.
- Studer, S., Hocke, K., and Kämpfer, N.: Intraseasonal oscillations of stratospheric ozone above Switzerland, *J. Atmos. Sol.-Terr. Phys.*, 74, 189–198, <https://doi.org/10.1016/j.jastp.2011.10.020>, 2012.
- Tschanz, B. and Kämpfer, N.: Signatures of the 2-day wave and sudden stratospheric warmings in Arctic water vapour observed by ground-based microwave radiometry, *Atmos. Chem. Phys.*, 15, 5099–5108, <https://doi.org/10.5194/acp-15-5099-2015>, 2015.
- Wu, D. L., Hays, P. B., and Skinner, W. R.: Observations of the 5-day wave in the mesosphere and lower thermosphere, *Geophys. Res. Lett.*, 21, 2733–2736, <https://doi.org/10.1029/94GL02660>, 1994.
- Yue, J., Liu, H.-L., and Chang, L. C.: Numerical investigation of the quasi 2 day wave in the mesosphere and lower thermosphere, *J. Geophys. Res.-Atmos.*, 117, D05111, <https://doi.org/10.1029/2011JD016574>, 2012.